Available online at www.sciencedirect.com

SciVerse ScienceDirect

Ceramics International 38 (2012) 5967–5971

CERAMICS INTERNATIONAL

www.elsevier.com/locate/ceramint

Dependence of the microstructure and properties of TiC/Ti_3SiC_2 composites on extra C addition

Jun Wang [a,b], Ai-Ju Li [a,b,*], Su-Mei Wang [a,b], Hai-Xia Zeng [c]

[a] Key Laboratory for Liquid-Solid Structural Evolution and Processing of Materials, Ministry of Education, Shandong University, Jinan 250061, PR China
[b] Engineering Ceramics Key Laboratory of Shandong Province, Shandong University, Jinan 250061, PR China
[c] School of Civil Engineering, Shandong University, Jinan 250061, PR China

Received 26 December 2011; received in revised form 15 April 2012; accepted 16 April 2012
Available online 22 April 2012

Abstract

TiC/Ti_3SiC_2 composites were synthesized with Ti/Si/C and Al (in which extra C addition ranges from 0 to 25 wt.%) as starting powders by hot-pressed sintering method at 1400 °C under 30 MPa. X-ray diffraction (XRD) and scanning electron microscopy (SEM) were used to evaluate the phase composition and the fracture surface. The results reveal that with the increase of extra C addition, the content of Ti_3SiC_2 phase decreases while the content of TiC phase increases. Graphite phase is detected in the samples with extra C addition of 20 wt.% and 25 wt.%. The bending strength decreases from 554.81 MPa to 57.44 MPa due to the decrease of the densification and Ti_3SiC_2 phase content. The electrical conductivity falls from 42,474.52 s/cm to 1524.95 s/cm, resulting from lower Ti_3SiC_2 phase content and higher contact resistance.

Keywords: B. Composites; C. Electrical conductivity; TiC/Ti_3SiC_2; Bending strength

1. Introduction

The MAX phases in the ternary compound family with the general formula $M_{n+1}AX_n$ (M is an early transition metal, A is an element of group IIIA or IVA, X is C and/or N and $n = 1–3$) have attracted considerable attention in the past decades [1,2]. Ti_3SiC_2 exhibits a crystal structure of a double Ti–C block separated by hexagonal nets of Si atoms [3]. It has been the subject of intensive research due to its unique characteristics, such as high electrical conductivities ($\sim 4.5 \times 10^6$ s/m) and thermal conductivities (~37 W/m K), low density (~4.53 g/cm^3), high melting point (~3000 °C), relatively high bending strength (~600 MPa), high thermal stability, excellent thermal shock resistance, high machinability and unusual damage tolerance [1,4–6].

Because of its high electrical conductivity, high flexural strength, high hardness, good erosion resistance and good thermal stability [7,8], TiC is one of the most promising candidates for high-temperature structural materials. Therefore, when it is allowed to combine with Ti_3SiC_2, the formation of a new kind of TiC/Ti_3SiC_2 composites is expected. The composites formed by such a combination may hold great promise for industrial application due to the advantages associated with the marriage of two components. Different technologies, such as mechanical alloying (MA) [9], hot isostatic pressing (HIP) [10], self-propagating high-temperature synthesis (SHS) [11], reactive sintering, pulse discharge sintering (PDS) [12], and spark plasma sintering (SPS) [13], have been developed to synthesize TiC/Ti_3SiC_2 composites during the past decades. To date, many raw materials were used to prepare the TiC/Ti_3SiC_2 composites, including Ti/Si/C/TiC/Al [10], TiC/Ti_3SiC_2 [11], TiH_2/SiC/TiC [12], Ti/Si/C/Al [13], Ti/SiC/C [14], Ti/Si/TiC system [15]. However, these starting materials require complex steps and high production cost to obtain them. In the present work, Ti/Si/C with a small amount of Al and extra C addition as starting powders were used to prepare TiC/Ti_3SiC_2 composites. Compared with the above methods, this approach was more affordable. The small amount of Al worked as sintering aims to accelerate the sintering and densification process of Ti_3SiC_2 bulk material [16]. The

* Corresponding author at: Key Laboratory for Liquid-Solid Structural Evolution and Processing of Materials, Ministry of Education, Shandong University, Jinan 250061, PR China. Tel.: +86 531 88392439; fax: +86 531 88395881.
E-mail address: liaiju57@sina.com (A.-J. Li).

0272-8842/$36.00.
http://dx.doi.org/10.1016/j.ceramint.2012.04.049

influence of extra C addition on the microstructure and physical properties of the composites was analyzed in detail.

2. Experimental

2.1. Samples preparation

Commercially available Ti (titanium, −200 mesh, ≥99%), Si (silicon, −200 mesh, ≥99%), C (graphite, −200 mesh, ≥95%) and Al (aluminum, −200 mesh, ≥99%) were purchased from PR China and selected as raw powders. Those starting powders were mixed in molar ratios of Ti:Si:C:Al = 3:1:2:0.2 with the weight percent of extra C addition ranging from 0 to 25 wt.%. The samples were labeled as S1–S6 in sequence to Ti_3SiC_2, Ti_3SiC_2–5 wt.%C, Ti_3SiC_2–10 wt.%C, Ti_3SiC_2–15 wt.%C, Ti_3SiC_2–20 wt.%C, Ti_3SiC_2–25 wt.%C, respectively.

The powders were mixed in a planetary high-energy ball miller for 2 h at the speed of 300 rpm under an Ar atmosphere. The mixed powders were compacted in a graphite mold with an inner size of 42 mm. The hot-pressed sintering synthesis process was performed in a multi-purpose high temperature furnace (High-Multi-5000, Fuji Denpa Kogyo Co., Ltd., Japan) at temperature of 1400 °C under pressure of 30 MPa for 60 min under an Ar atmosphere.

2.2. Phase and microstructure analysis

X-ray powder diffraction (XRD) patterns were obtained by an X-ray diffractometer (D/max-2400, Rigaku Corp., Japan) with Ni-filtered Cu Kα radiation ($V = 50$ kV, $I = 80$ mA). A scan rate of 4°/min and a step size of 0.02° were selected for a 2θ scan over the range of 10–80°. The fracture surface was observed using a scanning electron microscope (SEM, JSM-6610LV, JEOL, Japan).

2.3. Physical properties

The density of composites and water absorption rate were carried out using Archimede's method. Three-point bending tests were conducted to measure the bending strength using a CMT5105 type electromechanical universal testing machine with the displacement rate of 0.5 mm min^{-1}. Electrical conductivity of the samples was measured by a QJ44 type four-point probe instrument.

3. Results and discussion

3.1. Phase analysis

The X-ray diffraction patterns of the samples with different amount of extra C addition are shown in Fig. 1. All the XRD patterns indicate that the reaction system is mainly composed of two phases: TiC phase and Ti_3SiC_2 phase. With the increase of extra C addition, the intensity of TiC peaks increases while that of Ti_3SiC_2 peaks decreases. In the samples with extra C addition of 20 wt.% and 25 wt.%, the graphite peaks are detected.

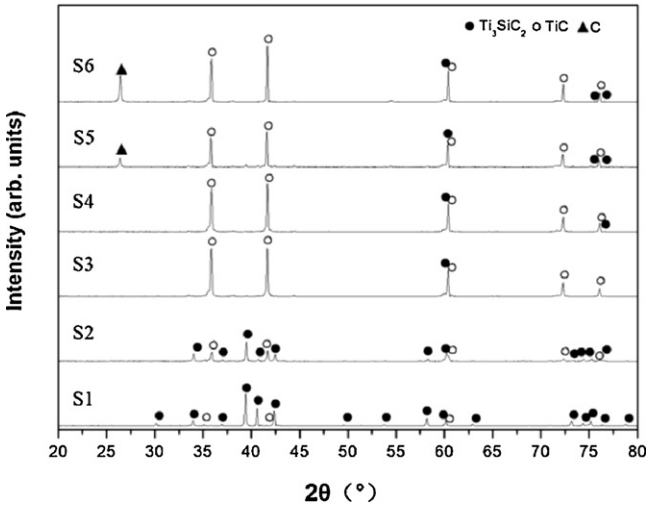

Fig. 1. X-ray diffraction patterns of TiC/Ti_3SiC_2 composites S1–S6.

In this experiment system, chemical reactions in the sintering process are listed as Eqs. (1)–(3). TiC phase forms firstly as reaction (1) takes place above 870 °C [17]. The eutectic liquid then appears at temperature near the eutectic point of Ti–Si (1330 °C), causing the formation of Ti_3SiC_2 phase at the interface between the eutectic liquid phase and the TiC particles [18].

$$Ti + C \rightarrow TiC \quad (1)$$

$$Ti + Si \rightarrow Ti{-}Si(L) \quad (2)$$

$$Ti{-}Si(L) + TiC \rightarrow Ti_3SiC_2 \quad (3)$$

Accurate quantification of phases requires reference patterns of the pure phases, but the relative weight percentage of different phase in the sintered samples can be compared to get an idea according to the fractional area under the peaks of various phases for given XRD patterns [19]. The calculated area under the peaks (in percentage of total area under the pattern) of various phases in different samples is listed in Table 1. The content of Ti_3SiC_2 phase seems to decrease unambiguously whereas the total content of TiC and graphite phase seems to increase.

It is noted that TiC, which is one of the products and intermediate phase in the synthesized composites, plays a significant role in the reaction process. With the increase of

Table 1
Calculated area under the peaks (in percentage of total area under the pattern) of various phases in different samples.

Sample	Ti_3SiC_2	TiC	Graphite
S1	93.7	6.3	–
S2	71.7	28.3	–
S3	21.7	78.3	–
S4	20.6	79.4	–
S5	20.3	69.1	10.6
S6	15.4	64	20.6

extra C addition, more TiC particles are formed based on reaction (1). Reactions (2) and (3) are hence repressed, resulting in the content of Ti_3SiC_2 phase to decrease accordingly. Meanwhile, graphite peaks do not appear in S1–S4 as extra C is low and therefore fully involved in the formation of TiC and Ti_3SiC_2. As the amount of C addition increases to an extent, C is fully reacted and super-saturated, leading to dramatic rise of graphite phase content in S5–S6. Decline of TiC phase content may be related to increasing proportion of excess graphite phase in the composite.

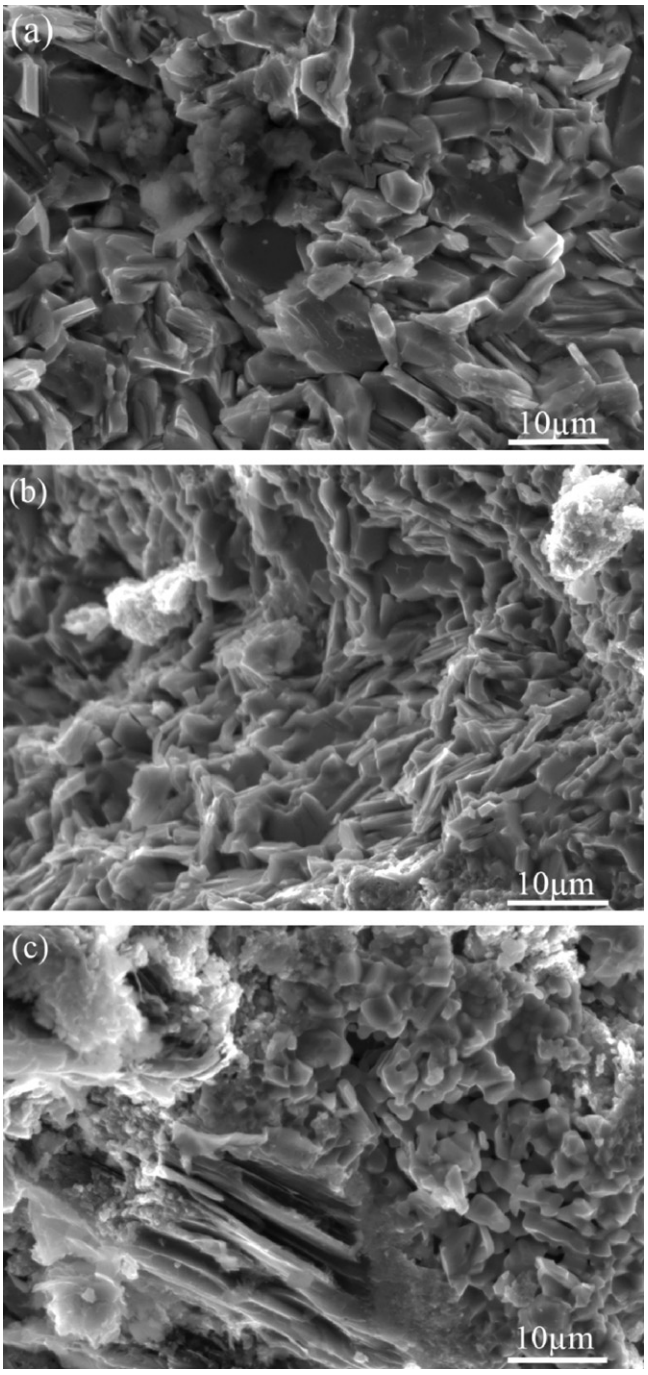

Fig. 2. SEM photographs of the fracture surface of (a) S1, (b) S2 and (c) S5.

3.2. Microstructure analysis

The SEM photographs of the fracture surface of S1, S2 and S5 are shown in Fig. 2. It is clear that the average grain size of the sample S1 is relatively large and that the plate-like grains coat the fine particles effectively (shown in Fig. 2(a)). With the increase of extra C addition, the samples become porous, and particles distribute more and more unevenly. A small amount of white agglomerates can be observed clearly in Fig. 2(b). As shown in Fig. 2(c), the amount of agglomerates and their size increases dramatically, resulting in appearance of noticeable laminated structures. Combined with the XRD results and similar observations which have been reported in [13,15], it is believed that layered grains are Ti_3SiC_2 grains; fine particles and agglomerates are TiC particles and the laminated structure in some region of Fig. 2(c) indicates the existence of graphite phase.

3.3. Physical properties

3.3.1. Effect of extra C addition on relative density and water absorption rate

The relative density and the water absorption rate of TiC/Ti_3SiC_2 composites with different extra C addition are shown in Fig. 3. The measured density of S1 is quite close to its theoretical value. Its water absorption rate, which is one of the methods for characterizing porosity of composites, is the lowest. With the increase of extra C addition, the relative density drops from 99.34% to 70.41%, while the water absorption rate increases from 0.12% to 2.98%. Decreasing content of layered Ti_3SiC_2 phase, along with increasing content of fine TiC phase and laminated graphite structure, leads to the decline of the densification level, which enhance the formation of more pores in the composites. Additionally, although the synthesis process was performed with flowing argon gas, it is possible for the air to enter into the reaction system. Due to the high reaction activity of O_2 and C at high temperature, gases such as CO and CO_2 could have formed, leading to the appearance of pores. The agglomerates and evaporation of Si in

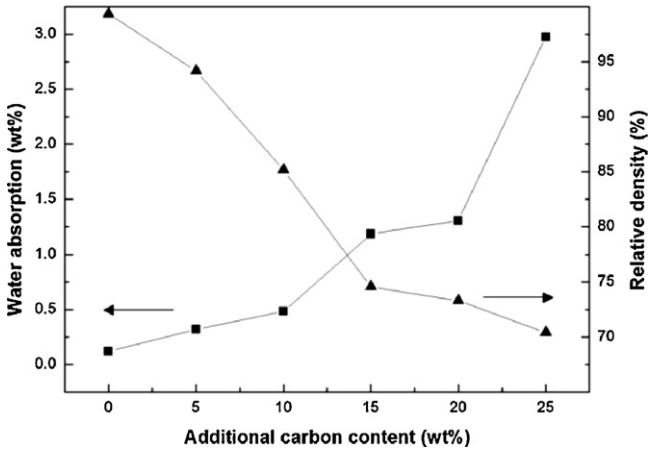

Fig. 3. The relative density and the water absorption rate of TiC/Ti_3SiC_2 composites with different amount of extra C addition.

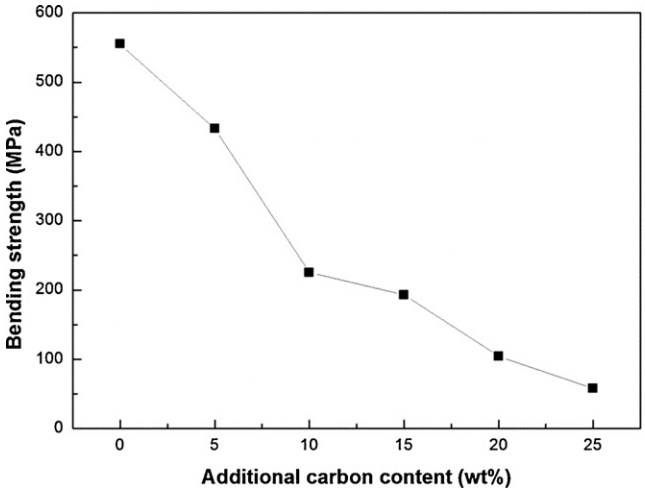

Fig. 4. The bending strength of TiC/Ti_3SiC_2 composites with different amount of extra C addition.

the experiment system [20] also lead to the generation of pores in the samples.

3.3.2. Effect of extra C addition on bending strength

The change in the bending strength with the increase of extra C addition is shown in Fig. 4. Bending strength of the composites reaches its maximum value of 554.81 MPa with none of extra C addition, and minimum value of 57.44 MPa with 25 wt.% of extra C addition, respectively. Significant decline of the densification which can be learnt in Fig. 3 is one of the dominating factors affecting the bending strength. With the increase of extra C addition, the samples appear from compact to porous and the densification decreases, so the bending strength strongly decreases. Besides, according to Table 1, it is obvious that the less Ti_3SiC_2 phase the sample contains, the lower the bending strength is. Because Ti_3SiC_2 has been proved to be a kind of damage-tolerant materials, it could consume the crack expansion energy via a number of multiple energy-absorbing mechanisms [21], which is helpful to redistribute the strain and dissipate the stress concentration. Additionally, the appearance of larger agglomerates makes crack propagate through the samples more easily, which will have a bad influence on the bending strength.

3.3.3. Effect of extra C addition on electrical conductivity

The variation of electrical conductivity with the different amount of C addition is shown in Fig. 5. It is worth noting that electrical conductivity of the composites drops from 42,474.52 s/cm to 1524.95 s/cm as the C addition increases from 0 to 25 wt.%. The movement of dislocated electrons in nets of Si atoms results in excellent conduction property of Ti_3SiC_2. Therefore Ti_3SiC_2 grains, as the main electrical channels, play an important role in the conduction process of the composite. As the content of Ti_3SiC_2 grains descends, the current carrier concentration decreases. Although TiC and C are all conductive, the theoretical electrical conductivity of C is around 10^{-2} times lower than that of Ti_3SiC_2, and the theoretical electrical conductivity of TiC is 1.60×10^4 s/cm

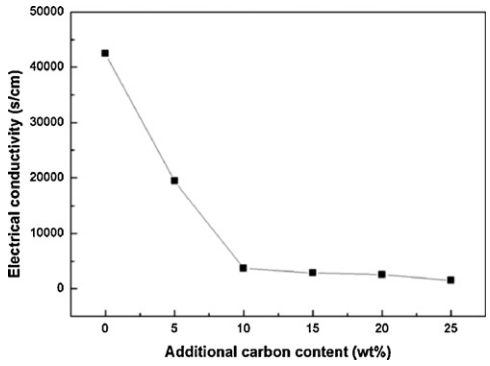

Fig. 5. The electrical conductivity of TiC/Ti_3SiC_2 composites with different amount of extra C addition.

[4]. It is not unreasonable to believe that the decrease of electrical conductivity is proportional to the variation of different phase content. Moreover, because the number of contact areas among the particles increases with the increase of TiC particles and C, which leads to higher contact resistance, the electrical conductivity decreases.

4. Conclusions

TiC/Ti_3SiC_2 composites were fabricated with Ti/Si/C and Al as starting powders by hot-pressed sintering technique at temperature of 1400 °C under pressure of 30 MPa. With the increase of extra C addition, the content of Ti_3SiC_2 phase decreases strongly whereas the total content of TiC and graphite phase increases. Graphite phase is detected in the samples with extra C addition above 20 wt.%. The relative density decreases from 99.34% to 70.41% and the water absorption rate increases from 0.12% to 2.98% due to decrease of the densification level. Decrease of the densification and Ti_3SiC_2 phase content can explain the decline of bending strength from 554.81 MPa to 57.44 MPa. Lower Ti_3SiC_2 phase content and higher contact resistance are responsible for the decline of the electrical conductivity from 42,474.52 s/cm to 1524.95 s/cm.

Acknowledgements

The authors would like to acknowledge Fenfen Fan and Xu Meng (Students of Key Laboratory for Liquid-Solid Structure Evolution and Processing of Materials, Ministry of Education) for their kind assistance and valuable suggestions during the process of the experiment.

References

[1] M.W. Barsoum, The $M_{N+1}AX_N$ phases: a new class of solids; thermodynamically stable nanolaminates, Progress in Solid State Chemistry 28 (2000) 201–281.
[2] M.W. Barsoum, H.I. Yoo, K.I. Polushina, Y.V. Rud, T. El-Raghy, Electrical conductivity thermopower, and Hall effect of Ti_3AlC_2, Ti_4AlN_3, and Ti_3SiC_2, Physical Review B 62 (2000) 10194–10198.
[3] T. Goto, T. Hirai, Chemically vapor deposited Ti_3SiC_2, Materials Research Bulletin 22 (1987) 1195–1201.

[4] M.W. Barsoum, T. El-Raghy, Synthesis and characterization of a remarkable ceramic – Ti_3SiC_2, Journal of the American Ceramic Society 79 (1996) 1953–1956.
[5] T. El-Raghy, M.W. Barsoum, A. Zavaliangos, S.R. Kalidindi, Processing and mechanical properties of Ti_3SiC_2. II: effect of grain size and deformation temperature, Journal of the American Ceramic Society 82 (1999) 2855–2860.
[6] Z.M. Sun, Z.F. Zhang, H. Hashimoto, T. Abe, Ternary compound Ti_3SiC_2. Part I: Pulse discharge sintering synthesis, Materials Transactions 43 (2002) 428–431.
[7] G.C. Wei, P.F. Becher, Improvements in mechanical properties in SiC by the addition of TiC particles, Journal of the American Ceramic Society 67 (1984) 571–574.
[8] L.J. Wang, W. Jiang, L.D. Chen, S.Q. Bai, Rapid reactive synthesis and sintering of submicron TiC/SiC composites through spark plasma sintering, Journal of the American Ceramic Society 87 (2004) 1157–1160.
[9] B.Y. Liang, X. Han, Q. Zou, Y.C. Zhao, M.Z. Wang, TiC/Ti_3SiC_2 composite prepared by mechanical alloying, International Journal of Refractory Metals and Hard Materials 27 (2009) 664–666.
[10] L.H. Ho-Duc, T. El-Raghy, M.W. Barsoum, Synthesis characterization of 0.3 Vf TiC–Ti_3SiC_2 0.3 Vf SiC–Ti_3 SiC_2 composites, Journal of Alloys and Compounds 350 (2003) 303–312.
[11] J. Lis, L. Chlubny, M. Łopaciński, L. Stobierski, M.M. Bućko, Ceramic nanolaminates—processing and application, Journal of the European Ceramic Society 28 (2008) 1009–1014.
[12] S. Konoplyuk, T. Abe, T. Uchimoto, T. Takagid, Synthesis of Ti_3SiC_2/TiC composites from TiH_2/SiC/TiC powders, Materials Letters 59 (2005) 2342–2346.
[13] J.F. Zhang, L.J. Wang, W. Jiang, L.D. Chen, Effect of TiC content on the microstructure and properties of Ti_3SiC_2–TiC composites in situ fabricated by spark plasma sintering, Materials Science and Engineering A 487 (2008) 137–143.
[14] T. El-Raghy, M.W. Barsoum, Processing and mechanical properties of Ti_3SiC_2. I: Reaction path and microstructure evolution, Journal of the American Ceramic Society 82 (1999) 2849–2854.
[15] W.B. Tian, Z.M. Sun, H. Hashimoto, Y.L. Du, Synthesis, microstructure and mechanical properties of Ti_3SiC_2–TiC composites pulse discharge sintered from Ti/Si/TiC powder mixture, Materials Science and Engineering A 526 (2009) 16–21.
[16] S.L. Yang, Z.M. Sun, Q.Q. Yang, H. Hashimoto, Effect of Al addition on the synthesis of Ti_3SiC_2 bulk material by pulse discharge sintering process, Journal of the American Ceramic Society 27 (2007) 4807–4812.
[17] R. Pampuch, M. Raczka, J. Lis, The role of liquid phase in solid combustion synthesis of Ti_3SiC_2, International Journal of Materials & Product Technology 10 (1995) 316–324.
[18] F. Sato, J.F. Li, R. Watanabe, Reaction synthesis of Ti_3SiC_2 from mixture of elemental powder, Materials Transactions 41 (2000) 605–608.
[19] A. Singh, S.R. Bakshi, D.A. Virzi, A.K. Keshri, A. Agarwal, S.P. Harimkar, In situ synthesis of TiC/SiC/Ti_3SiC_2 composite coatings by spark plasma sintering, Surface and Coatings Technology 205 (2011) 3840–3846.
[20] Z.M. Sun, S.L. Yang, H. Hashimoto, Ti_3SiC_2 power synthesis, Ceramics International 30 (2004) 1873–1877.
[21] S.B. Li, J.X. Xie, J.Q. Zhao, L.T. Zhang, Mechanical properties and mechanism of damage tolerance for Ti_3SiC_2, Materials Letters 57 (2002) 119–123.